Volume 56
Number 23
21 March 2020
Pages 3351–3462

# ChemComm

Chemical Communications

rsc.li/chemcomm

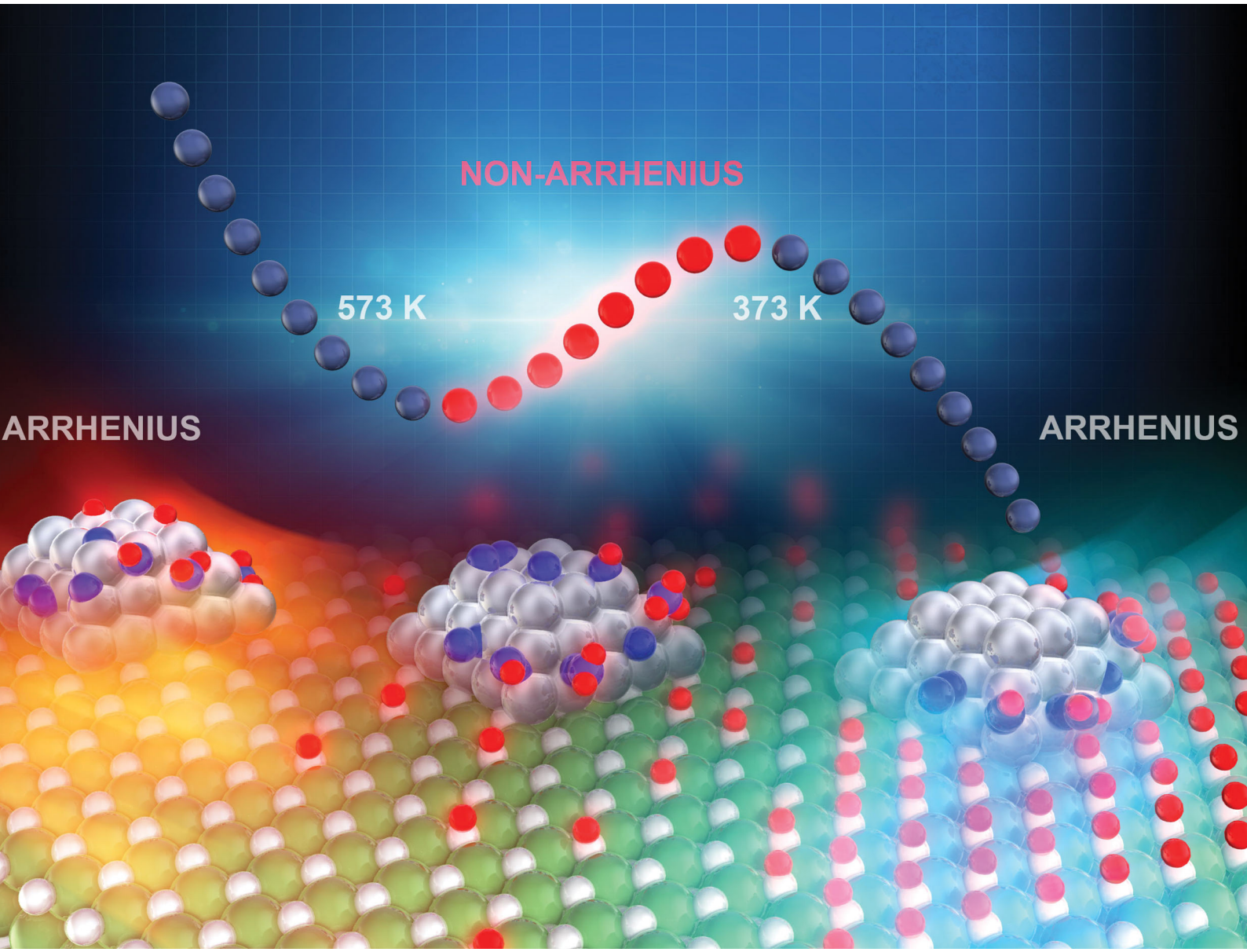


ISSN 1359-7345

ROYAL SOCIETY OF CHEMISTRY

**COMMUNICATION**

Yasushi Sekine *et al.*

Key factor for the anti-Arrhenius low-temperature heterogeneous catalysis induced by $H^+$ migration: $H^+$ coverage over support

ChemComm

COMMUNICATION

View Article Online
View Journal | View Issue



Cite this: *Chem. Commun.*, 2020, **56**, 3365

Received 18th January 2020,
Accepted 25th February 2020

DOI: 10.1039/d0cc00482k

rsc.li/chemcomm

# Key factor for the anti-Arrhenius low-temperature heterogeneous catalysis induced by $H^+$ migration: $H^+$ coverage over support†

Kota Murakami,[a] Yuta Tanaka,[a] Ryuya Sakai,[a] Yudai Hisai,[a] Sasuga Hayashi,[a] Yuta Mizutani,[a] Takuma Higo,[a] Shuhei Ogo,[a] Jeong Gil Seo,[b] Hideaki Tsuneki[a] and Yasushi Sekine *[a]

**Low-temperature heterogeneous catalytic reaction in an electric field is anticipated as a novel approach for on-demand and small-scale catalytic processes. This report quantitatively reveals the important role of proton coverage on the catalyst support for catalytic ammonia synthesis in an electric field, which shows an anti-Arrhenius behaviour.**

During the past several decades, industrial catalytic processes have been optimized for large-scale processes. They are operated efficiently under harsh conditions (high temperatures and pressures) using various facilities such as heat exchangers. However, for next-generation catalytic processes supporting a sustainable society, small-scale plants that work under milder conditions are anticipated for on-site and on-demand operation. To moderate catalyst working conditions, catalytic reactions using external stimuli (*e.g.* photonic, magnetic, and electric fields) have attracted great attention.[1–8] Our group, which has specifically examined the use of an electric field for low-temperature catalysis, has facilitated various catalytic reactions such as steam reforming of hydrocarbon, dehydrogenation of methylcyclohexane (MCH), and $NH_3$ synthesis.[9–23] In an electric field, $H^+$ hopping *via* surface hydroxyl groups proceeds (so-called surface protonics), thereby enabling the reaction path through collision between $H^+$ over support and adsorbent over loading metals such as $CH_4$, MCH, and $N_2$.

Various analyses have revealed novel catalysis qualitatively in an electric field induced by $H^+$ hopping.[9–23] Quantitative evaluation of the $H^+$ contribution to the overall reaction rate is extremely important. The work described herein succeeded in formulizing the effect of $H^+$ amount over supports in the electric field using $NH_3$ synthesis and $Ru/CeO_2$ respectively as a model reaction and catalyst.

For this study, 1 wt%$Ru/CeO_2$ was prepared using an impregnation method with $CeO_2$ (JRC-CEO-01) as a support. The effects on the $NH_3$ synthesis rate ($r$) were observed when using an electric field (6 mA direct current) and $H_2$ partial pressure ($P_{H_2}$) at various catalyst bed temperatures. Before all activity tests, the catalyst was pre-reduced under a common condition ($N_2:H_2$ = 1:3 ($P_{H_2}$ = 0.75 atm), 723 K, 2 h). A schematic image of the fixed-bed type reactor is presented in Fig. S1 (ESI†). The catalyst bed temperature was detected directly using a thermocouple attached on the catalyst particles to exclude Joule heat effects on the reaction caused by the imposed current.

Without the electric field, a conventional-shaped Arrhenius plot was obtained (open symbols in Fig. 1(a)). In contrast, the electric field induced completely different temperature dependence of the $NH_3$ synthesis rate (closed symbols in Fig. 1(a) and Tables S1, S2, ESI†). Conventional Arrhenius-like behaviour was detected in the high-temperature region (573–673 K). However, the slope decreased with the temperature decrement. Also, anti-Arrhenius-like behaviour emerged around 373–573 K. Subsequently, Arrhenius-like behaviour was confirmed again at temperatures lower than around 373 K. This peculiar trend suggests a change in the reaction mechanism depending on the catalyst bed temperature. The $P_{H_2}$ dependence supported this assumption (Fig. 1(b) and Tables S3–S6, ESI†). At around 373–573 K,

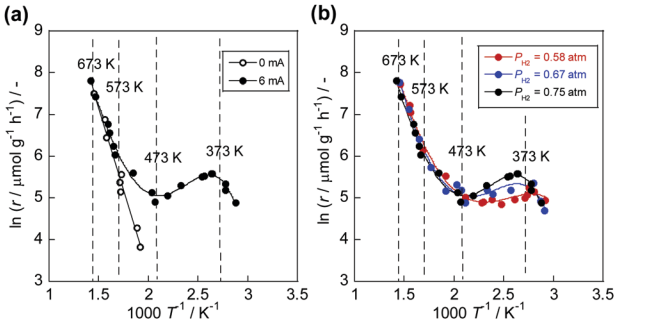


Fig. 1 Arrhenius plots for $NH_3$ synthesis rate ($r$) over 1 wt%$Ru/CeO_2$: (a) with/without the electric field (0 or 6 mA) under $P_{H_2}$ = 0.75 atm; and (b) $P_{H_2}$ dependence in the electric field (0.58, 0.67, and 0.75 atm) with 6 mA.

[a] *Department of Applied Chemistry, Waseda University, 3-4-1, Okubo, Shinjuku, Tokyo, 169-8555, Japan. E-mail: ysekine@waseda.jp*

[b] *Department of Energy Science and Technology, Myongji University, Nam-dong, Cheoin-gu, Yongin-si, Gyeonggi-do 449-728, South Korea*

† Electronic supplementary information (ESI) available. See DOI: 10.1039/d0cc00482k

at which anti-Arrhenius-like behaviour was observed, $P_{H_2}$ has a positive effect on the reaction rate, although the reaction rates changed slightly at other temperature regions. Conventionally, Ru-based catalysts show negative dependence on $P_{H_2}$ because of $H_2$ poisoning over the Ru surface.[24–26] When the $CeO_2$ is used as the support, the poisoning is suppressed by virtue of the spillover of H atom from Ru surface to $CeO_2$.[27] Without the electric field, we also confirmed a slight change of activities with increasing $P_{H_2}$ (Fig. S2, ESI†). Therefore, enhancement of the activities by high $P_{H_2}$ over $Ru/CeO_2$ is a completely specific trend in the electric field, indicating a novel reaction mechanism.

Reportedly, conventional ammonia synthesis proceeds *via* the 'dissociative mechanism', where supplied $N_2$ directly dissociates.[28]

$$N_2 \rightarrow 2N_{ad} \quad (1)$$

$$H_2 \rightarrow 2H_{ad} \quad (2)$$

$$N_{ad} + 3H_{ad} \rightarrow NH_{3(g)} \quad (3)$$

However, most recently, we have inferred that ammonia synthesis in the electric field proceeds through the 'associative mechanism', where $N_2$ associates with $H^+$ over supports before dissociation.[19]

$$H_2 \rightarrow 2H_{ad} \quad (4)$$

$$H_{ad} \rightarrow H^+_{ad} + e^- \quad (5)$$

$$N_{2ad} + H^+_{ad} + e^- \rightarrow N_2H_{ad} \quad (6)$$

$$N_2H_{ad} + H^+_{ad} + e^- \rightarrow N_2H_{ad} \quad (7)$$

$$N_2H_{2ad} + H^+_{ad} + e^- \rightarrow N_{ad} + NH_{3(g)} \quad (8)$$

Here, 'ad' denotes adsorbed species, and '*g*' means gaseous species. In addition, $N_xH_y$ ($x$ = 0–2, $y$ = 0–2) adsorbs over loaded metals and $H^+$ adsorbs over lattice oxygen of supports ($O_{lat}$). Similarly, we have reported C–H cleavage activation by hopping proton over a support.[9–18] Therefore, the amount of $H^+$ over the support is expected to be crucially important for novel catalysis in the electric field. We assumed, therefore, that the temperature dependence of the $H^+$ coverage over $CeO_2$ plays an important role in specific temperature dependence with the electric field.

To elucidate this hypothesis quantitatively, the temperature dependence of $H^+$ coverage over $O_{lat}$ under $P_{H_2}$ = 0.75 atm was investigated using *in situ* FT-IR measurements in a transmission mode (Fig. 2(a)) without the electric field and DRIFTs mode (Fig. 2(b)) with/without the electric field. The hydrogen adsorption energy over $O_{lat}$ ($H^+$ stability over $O_{lat}$) was fundamentally important for the $NH_3$ synthesis rate in the electric field.[19] To exclude effects of atmospheric $H_2O$ outside of the measurement cell, $D_2$ was supplied as a reactant. Also, $O_{lat}$-$D^+$ stretching peaks (around 2780 $cm^{-1}$)[29] were used for *pseudo*-quantitative analysis of the $H^+$ amount at each temperature. Detailed measurement procedures are shown in Fig. S3 (ESI†). The IR cell for transmission mode is suitable for a quantitative investigation of surface OH group (Fig. 2(c)), on the other hand the electric field is not applicable for the cell due to its structure. So we also measured DRIFTs for evaluating the effect of the electric field on the amount of surface OH group (note that DRIFTs cannot evaluate the precise quantitative amount due to its principle). The qualitative

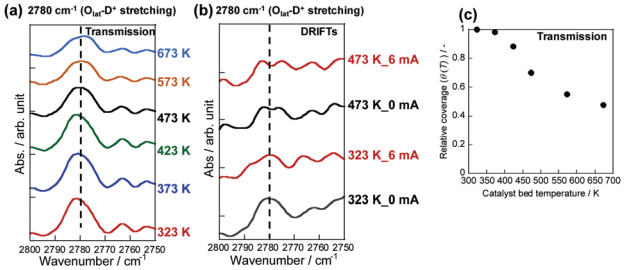


Fig. 2 Quantitative analysis for $O_{lat}$-$D^+$ over 1 wt%$Ru/CeO_2$ under $N_2$ 5 SCCM and $D_2$ 15 SCCM: (a) *in situ* IR transmission spectra, (b) *in situ* IR DRIFTs spectra with/without EF, and (c) relative coverage by transmission spectra ($\theta(T)$ = Area($T$)/Area(323 K)).

analysis with the electric field (Fig. 2(b)) showed that no significant change was observed by the application of electric field. Electric field application produces small amount of Joule heat, so small change can be observed, but the effect of gas phase temperature (*i.e.* difference in between 323 K and 473 K) on the adsorption is much larger.

We calculated the relative coverage of $H^+$ ($\theta(T)$) using the peak area, where the value at 323 K (Area (323 K)) was used as a reference (eqn (9)).

$$\theta(T) = \text{Area}(T)/\text{Area}(323\ \text{K}) \quad (9)$$

Results revealed that the $H^+$ coverage decreased with the increment in temperatures (Fig. 2(c)). Furthermore, at 323–373 K, the $H^+$ coverage changed slightly, indicating saturation of $H^+$ coverage.

The obtained $\theta(T)$ suggested the contribution of $H^+$ coverage dependence on the temperature to the specific Arrhenius plots in the electric field. When catalyst bed temperatures are higher than 573 K, the decrement in $H^+$ over $CeO_2$ renders the $NH_3$ synthesis rate acceleration negligible, which means that $NH_3$ synthesis at the high-temperature region proceeds *via* a conventional 'dissociative mechanism'. Fig. 2 reveals that the $O_{lat}$-$D^+$ remained on the surface to some extent even at high temperature region, however, the influence became small from following reasons. At first, the reaction through 'dissociative mechanism' is much active at high temperature region. Furthermore, the 'associative mechanism' is limited at the three phases boundary (TPB),[22] although the 'dissociative mechanism' can proceed over all region of metal surface. It means that the reaction site for 'dissociative mechanism' is much larger than that for 'associative mechanism'. Therefore, the contribution of 'associative mechanism' to the overall reaction rate became very small at high temperature region even if there is proton over supports. In contrast, the $CeO_2$ surface is covered by $H^+$ sufficiently at temperatures lower than 373 K; also, $H^+$ reacts with $N_2$ over Ru. The overall reaction rate at around 373–573 K can be described as the sum of two rates of reaction through the 'dissociative mechanism' and the 'associative mechanism.' Therefore, we assumed that the overall $NH_3$ synthesis rate in the electric field is definable as

$$r_{calc}(T) = r_{dissociative}(T) + \theta(T) \times r_{associative}(T) \quad (10)$$

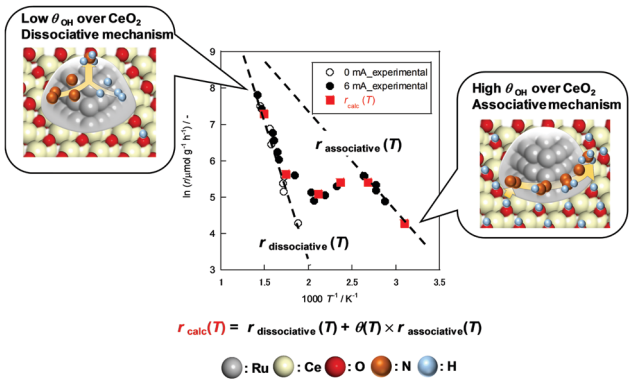


Fig. 3 Experimental reaction rate under $P_{H_2}$ = 0.78 atm and calculated reaction rate ($r_{calc}(T)$). Data in Fig. 1(a) are used for $r_{dissociative}$ and $r_{associative}$.

where $r_{dissociative}(T)$ and $r_{associative}(T)$ show the extrapolated values (Fig. 3). The Arrhenius plots without the electric field (Fig. 1(a)) are used for $r_{dissociative}(T)$. $r_{associative}(T)$ was calculated using approximate straight line which was drawn using experimental values at low-temperature ($T < 373$ K) region. At the region, negligible change of $\theta(T)$ was detected, and Arrhenius-like behaviour was confirmed for $NH_3$ synthesis rate in the electric field. Therefore, we concluded that the straight line at right side in Fig. 3 would mean the ideal $NH_3$ synthesis rate through 'associative mechanism' with maximum $H^+$ coverage. Rate determining step (RDS) approximation was used for the second term of the eqn (10). We inferred that the RDS in the electric field might be the $N_2H$ formation step (eqn (6)), meaning that the reaction rate would be scaled linearly by the $H^+$ concentration.[19] As for the $H^+$ concentration, the actual measured values presented in Fig. 2(c) are used. Fig. 3 shows a comparison between $r_{calc}(T)$ and the experimental value. For this consideration, $r$ under $P_{H_2}$ = 0.75 atm with 6 mA was used. It is particularly interesting that the calculated value showed close agreement with the experimental value. The coincidence reveals the linear correlation between the enhancement of the reaction rate and $H^+$ amount in the electric field. It also supports the credibility of RDS approximation on $N_2H$ formation step. This result also corresponds to the $P_{H_2}$ dependence shown in Fig. 1(b). The temperature of inflection points around 373 K became lower. Under $P_{H_2}$ = 0.78 atm, the $H^+$ coverage hits ceiling at around 373 K, and the conventional temperature dependence emerged. When the $P_{H_2}$ decreased, the temperature at which reaches a limit became lower owing to the decrease of $H^+$ source.

This report is the first study that quantitatively assesses the relation between $H^+$ coverage and reaction rates in the electric field. This finding is expected to be expanded to other reaction systems involving $H^+$ and is expected to constitute an essential guideline for the optimization of catalyst and reaction conditions in an electric field. For instance, when the reaction was conducted in a low-$P_{H_2}$ atmosphere, catalysts should be designed to keep $H^+$ tightly. In contrast, under high $P_{H_2}$, catalysts that bind $H^+$ loosely would be demanded to enhance the $H^+$ supply ability.[19]

In summary, we analysed the novel catalysis quantitatively and qualitatively under an electric field using $NH_3$ synthesis as a model reaction. We identified a peculiar temperature dependence of the $NH_3$ synthesis rate in the electric field. Three regions were confirmed: anti-Arrhenius-like behaviour emerged at around 373–573 K; Arrhenius-like behaviour was observed in the other two temperature regions ($T > 573$ K or $T < 373$ K). Furthermore, $P_{H_2}$ dependence on the electric field was influenced by the temperature. The activities increase with high $P_{H_2}$ only around 373–573 K. The $H^+$ coverage was detected using *in situ* FT-IR measurements in a transmission mode. The results of analysis showed that the increment of $H^+$ coverage accorded to the temperature decrease. The coverage hits a ceiling at around 373 K. Based on the findings described above, the overall reaction rate in the electric field was formulated. The calculated reaction rate fitted closely to the experimental values. The linear relation between the $H^+$ coverage and enhancement of the reaction rate by the electric field are indicated clearly. These insights are fundamentally important for the further investigation of catalytic reactions in the electric field.

This study was supported by JST MIRAI.

## Conflicts of interest

The authors have no conflict to declare related to this paper.

## Notes and references

1 A. Iwase and A. Kudo, *Chem. Commun.*, 2017, **53**, 6156–6159.
2 J. Xu, C. Pan, T. Takata and K. Domen, *Chem. Commun.*, 2015, **51**, 7191–7194.
3 F. Che, J. T. Gray, S. Ha and J. S. McEwen, *ACS Catal.*, 2017, **7**(10), 6957–6968.
4 A. Yamamoto, S. Mizuba, Y. Saeki and H. Yoshida, *Appl. Catal., A*, 2016, **521**, 125–132.
5 M. Iwamoto, M. Akiyama, K. Aihara and T. Deguchi, *ACS Catal.*, 2017, **7**, 6924–6929.
6 Y. Kobayashi, N. Shimoda, Y. Kimura and Y. Satokawa, *ECS Trans.*, 2017, **75**(42), 43–52.
7 L. Zhang, L. X. Ding, G. F. Chen, X. Yang and H. Wang, *Angew. Chem., Int. Ed.*, 2019, **58**, 2612–2616.
8 T. Nozaki, N. Muta, S. Kado and K. Okazaki, *Catal. Today*, 2004, **89**(1–2), 57–65.
9 M. Torimoto, K. Murakami and Y. Sekine, *Bull. Chem. Soc. Jpn.*, 2019, **92**(10), 1785–1792.
10 M. Torimoto, S. Ogo, D. Harjowinoto, T. Higo, J. G. Seo, S. Furukawa and Y. Sekine, *Chem. Commun.*, 2019, **55**, 6693–6695.
11 S. Okada, R. Manabe, R. Inagaki, S. Ogo and Y. Sekine, *Catal. Today*, 2018, **307**, 272–276.
12 R. Manabe, S. Okada, R. Inagaki, K. Oshima, S. Ogo and Y. Sekine, *Sci. Rep.*, 2016, **6**, 38007.
13 T. Yabe, K. Yamada, T. Oguri, T. Higo and Y. Sekine, *ACS Catal.*, 2018, **8**, 11470–11477.
14 R. Inagaki, R. Manabe, Y. Hisai, Y. Kamite, T. Yabe, S. Ogo and Y. Sekine, *Int. J. Hydrogen Energy*, 2018, **43**(31), 14310–14318.
15 K. Takise, A. Sato, K. Muraguchi, S. Ogo and Y. Sekine, *Appl. Catal., A*, 2019, **573**, 56–63.
16 M. Kosaka, T. Higo, S. Ogo, J. G. Seo, K. Imagawa, S. Kado and Y. Sekine, *Int. J. Hydrogen Energy*, 2020, **45**(1), 738–743.
17 K. Takise, A. Sato, S. Ogo, J. G. Seo, K. Imagawa, S. Kado and Y. Sekine, *RSC Adv.*, 2019, **9**, 27743–27748.
18 K. Takise, A. Sato, K. Murakami, S. Ogo, J. G. Seo, K. Imagawa, S. Kado and Y. Sekine, *RSC Adv.*, 2019, **9**, 5918–5924.
19 K. Murakami, Y. Tanaka, S. Hayashi, R. Sakai, Y. Hisai, Y. Mizutani, A. Ishikawa, T. Higo, S. Ogo, J. G. Seo, H. Tsuneki, H. Nakai and Y. Sekine, *J. Chem. Phys.*, 2019, **151**, 064708.
20 K. Murakami, Y. Tanaka, R. Sakai, K. Toko, K. Ito, A. Ishikawa, T. Higo, T. Yabe, S. Ogo, M. Ikeda, H. Tsuneki, H. Nakai and Y. Sekine, *Catal. Today*, DOI: 10.1016/j.cattod.2018.10.055.

21 K. Murakami, R. Manabe, H. Nakatsubo, T. Yabe, S. Ogo and Y. Sekine, *Catal. Today*, 2018, **303**, 271–275.
22 A. Gondo, R. Manabe, R. Sakai, K. Murakami, T. Yabe, S. Ogo, M. Ikeda, H. Tsuneki and Y. Sekine, *Catal. Lett.*, 2018, **148**(7), 1929–1938.
23 R. Manabe, H. Nakatsubo, A. Gondo, K. Murakami, S. Ogo, H. Tsuneki, M. Ikeda, A. Ishikawa, H. Nakai and Y. Sekine, *Chem. Sci.*, 2017, **8**, 5434–5439.
24 K. Aika, A. Ohya, A. Ozaki, Y. Inoue and I. Yasumori, *J. Catal.*, 1985, **92**, 305–311.
25 H. Bielawa, O. Hinrichsen, A. Birkner and M. Muhler, *Angew. Chem., Int. Ed.*, 2001, **40**(6), 1061–1063.
26 S. E. Siporin and R. J. Davis, *J. Catal.*, 2004, **225**, 359–368.
27 Y. Niwa and K. Aika, *Chem. Lett.*, 1996, 3–4.
28 K. Honkala, A. Hellman, I. N. Remediakis, A. Logadottir, A. Carlsson, S. Dahl, C. H. Christensen and J. K. Nørskov, *Science*, 2005, **307**, 555–558.
29 K. Werner, X. Weng, F. Calaza, M. Sterrer, T. Kropp, J. Paier, J. Sauer, M. Wilde, K. Fukutani, S. Shaikhutdinov and H. J. Freund, *J. Am. Chem. Soc.*, 2017, **139**(48), 17608–17616.